SEPARATION AND QUANTIFICATION OF AIRFOIL LE- AND TE-NOISE SOURCE WITH MICROPHONE ARRAY*

Weiyang Qiao, Liang Ji, Fan Tong, Liangfeng Wang and Weijie Chen
School of Power and Energy, Northwestern Polytechnical University
West Youyi Road 127#, 710072, Xi'an, China

ABSTRACT

The present paper concerns the separation and quantification of airfoil LE and TE noise source in an indoor open jet wind tunnel test. A linear array of 32 microphones was used in this program to determine the leading-edge and trailing-edge noise of airfoil. With the Clean-SC approach and with the correction of reverberation and shear layer, the background noises produced by the wind tunnel exit jet is successfully removed using the removing of Cross Spectral Matrices(CSM_{back}) of the background noises from the *CSM* of measurement noise. Clear and quantitative sound radiation results from the airfoil LE and TE noise source are obtained. The test results of LE and TE noise are related to the flow velocity and compared to the Amiet's and Howe's edge noise theory prediction. There is a good coincidence between present test results and classical aeroacoustic theory for the LE and TE edge noise at the attack angle of zero degree. It is found that overall sound pressure level (OASPL) varies approximately as U6.5 and U5.1 for the leading edge noise and trailing edge noise respectively when flow attack angle is zero degree. The LE noise SPL of airfoil is decreased with increase of attack angle. The largest difference of the SPL between LE noise at -10degree and +10degree is about 5dB. However, the TE noise has a complicated relation with the airfoil attack angle. It was found that the TE noise SPL is largest at the attack angle of -5degree in the test flow speed range, especially at the frequency range above 2000Hz. The test data indicated the influence of the flow attack angle on the trailing edge noise is greater than that on leading edge noise. The OASPL of LE noise varies with the airflow speed by the exponential relationship with the small index range of 5.965~6.486, and the OASPL of TE noise varies with the airflow speed by the exponential relationship with a very large index range of 3.138~6.244.

1 INTRODUCTION

The reduction of the turbulence broadband noise from the trailing-edge (TE) and leading-edge(LE) of airfoil or the turbomachinery blade is nowadays an important industrial need and probably one of the most challenging issues in aero-acoustics. LE noise which results from

* Project 51276149 and project 51476134 supported by National Natural Science Foundation of China.

the interaction of inflow turbulence and the airfoil/blade leading-edge, and TE noise which results from the interaction between the turbulent boundary layers that grow on the airfoil/blade and the sharp trailing edge.

Trailing-edge noise and leading-edge noise have been studied by many researchers. Being cognizant of an overestimate in the case of the infinite plane and an underestimate in the case of the hard semi-infinite plane for the edge noise with the simple application of Curle's theory[1], considerable progress has been made towards a clarification of various surface effects. In such case, the relevant length and velocity scales of flow field are affected by the sharp edge, and the edge acting as scattering centers in the vicinity of which the field is governed by diffraction effects according to linearized propagation equations. Powell (1960) firstly studied the trailing edge noise[2]. It was deduced from this model that the edge noise sound power varies approximately as U4.6. However, Powell's treatment was not sufficiently detailed to predict the field shape of radiation, nor could the effects of flight be considered. The first essential results and theoretical understanding of the trailing-edge problem is due to Ffowcs Williams and Hall (1970)[3]. Based on the solution of Lighthill' acoustic analogy equation with an appropriate Green's function, they showed that the far-field intensity of the sound field produced by turbulence past trailing edge varies with θ as $\sin^2(\theta/2)$ and scales with a typical flow velocity U as U5. After Ffowcs Williams and Hall, many researchers worked on edge noise to understand and predict of this noise, such as Crighton & Leppington 1970[4], Crighton 1972[5], Chandiramani 1974[6], Levine 1975[7], Howe 1975, 1976[8.9], Chase 1972,1975[10,11], Davis 1975[12]. A fairly satisfactory theoretical understanding of the trailing-edge noise problem has been achieved with Howe's review (1978)[13] in which numerous partially overlapping, partially conflicting theoretical approaches are reconciled and generalized to include a number of effects.

However, the present aeroacoustic theory of TE noise and LE noise does not meet the needs of the reduction of the turbulence broadband noise of airfoil or the turbomachinery blade. For example, it is found that Howe's theoretical model over-predicted very large noise reduction levels with serrated trailing-edge in some frequency, and lowly-predicted very much the noise suppression with serrated trailing-edge in other frequency range[14]. It is proposed that the flow and acoustic mechanism of the real airplane wing and turbomachinery blade are more sophisticated than that of semi-infinite plane due to the elaborate loading distribution, flow turn, the change of flow attack angle in the real blade. Especially, there is a complicated interrelationship between leading-edge flow and trailing-edge flow for the real blade due to the small chord[14].The LE noise source and TE noise source always arise simultaneously, and these two sources are always very closer each other in real blade. In order to understand the mechanism of LE and TE noise, and to evaluate the noise reduction of the airfoil and blade turbulence noise, it is necessary to separate and quantify the airfoil LE and TE noise source in the experimental research. Especially, because the most aerodynamics and performance tests are mostly carried out in the indoor test-bed, and not all aeroacoustic test could be done in a perfect anechoic room. There will be very strong background noise which will contaminate the LE and TE noise radiation in these tests. It would be significant to separate and quantify the airfoil LE and TE noise source to get the useful aeroacoustic information.

Modern microphone array was invented by Billingsley in 1974[15] and has since seen dramatic improvements due to the availability of better data acquisition and computing hardware. Recent mathematical and software developments invert the beamforming process and allow a quantitative determination of the sources. Beamforming is indispensable for the

localization of sound sources on moving objects, on flying aircraft, on high-speed trains, on motor cars in motion, on open rotors like helicopter and wind turbine rotors[16]. The beamforming maps are the result of a convolution of the point sources with the point-spread function [17]. The sound pressure levels of the maps are only reliable for point sources if the source positions have a sufficiently large separation. However, the sources along a line or distributed over an area or over a source volume yield results that depend on the beam width of the point-spread function. The consequence is that amplitudes of sound sources are very difficult to derive from beamforming maps and require experience. There are some attempts to achieve quantitative results by integrating certain regions of the map. The source levels of the point sources can be determined if the invert the convolution to be done. The result would be a set of point sources. In order to do this the point spread function of the array has to be calculated for every possible source position and for each narrow-band frequency of interest. The source levels of the unknown sources have then to be determined with a least square fit with the condition that only positive source levels are permitted. This deconvolution yields huge and badly conditioned matrices and the special iterative procedures are required to solve them.

Dougherty and Stoker (1998) developed the simpler version of the CLEAN algorithm, and firstly used this invert method in aeroacoustic sources identification [18]. Here the point spread function of only the strongest source is calculated and the model maps for small point sources located in the peak position of the map are successively subtracted from the beamforming map, which is cleaned by this procedure from all the side-lobes connected with the main lobe. However, the method works only well in the case of a few well localized sources. A first procedure proposed to solve the complete inverse problem was published by Brühl and Röder (2000) [19]. Brooks and Humphreys[20-22] firstly published the Deconvolution Approach for the Mapping of Acoustic Sources (DAMAS) about the phased microphone arrays in 2004. For the past years, deconvolution is an extensively studied topic in the field of aero-acoustic source identification where the sound generated by flow turbulence presents a distributed coherent source region, which challenges the localization accuracy of Conventional Beamforming[23-26]. Typical examples are CLEAN-SC (Sijtsma, 2007)[23], DAMAS-C (Brooks and Humphreys, 2006)[24], DAMAS2 (Dougherty, 2005)[25] and the Generalized Inverse Beamforming (GIBF, Suzuki, 2008) method[26], each having their advantages and drawbacks.

The present paper concerns the separation and quantification of airfoil LE and TE noise source in an indoor open jet wind tunnel test. In this study, a linear array of 32 microphones was used in this program to determine the leading-edge and trailing-edge noise of airfoil. The source identification technology based on the inverse method, Clean-SC approach with microphone array in free field, is improved and used to deal with the problems generated by acoustic measurement in normal test bed. The influences of reverberation and shear layer correction are all considered and corrected in this study. The background noises produced by the wind tunnel exit jet is successfully removed using the removing of Cross Spectral Matrices(CSM_{back}) of the background noises from the *CSM* of measurement noise. Based on the present method, the LE and TE noise sources of airfoil with high background noise are identified successfully. Clear and quantitative sound radiation results from the airfoil LE and TE noise source are obtained. The test results of LE and TE noise are related to the flow velocity and compared to the Amiet's and Howe's edge noise theory prediction, there is a good coincidence between present test results and classical aeroacoustic theory. It is found that overall sound pressure level (OASPL) varies approximately as U6.5 and U5.1(U is the

mean flow velocity) for the leading edge noise and trailing edge noise respectively when flow attack angle is zero degree. It is found that, when the flow attack angle is changed, the OASPL of LE noise varies with the airflow speed by the exponential relationship with the small index range of 5.965~6.486. However, the OASPL of TE noise varies with the airflow speed by the exponential relationship with a very large index range of 3.138~6.244.

2 EXPERIMENTAL SET-UP

The experiment was carried out in the low speed open jet wind tunnel in Northwestern Polytechnical University, and the SD2030 airfoil is tested. The wind tunnel can be broken up into two major sections: the upstream section and the test section. The upstream section consists of the centrifugal fan, the settling screens, the diffuser and the contraction. Flow is supplied to the tunnel through a centrifugal fan which is powered by a 20 Kw AC motor. After passing through the fan, the flow is slowed down through a diffuser before entering the settling chamber. The total length of the diffuser and the settling chamber is about 2 m while the expansion ratio from the exit of the fan to the settling chamber is 1:5.75. Before exiting the settling chamber and entering the contraction, the flow passes through flow conditioning screens to reduce the turbulence levels and swirling. The contraction, with a contraction ratio of 1:8.22 directs the flow into the test section. The test section(as shown in figure 1), the open jet of wind tunnel exit with a 0.3 m×0.09 m rectangular channel. Air is supplied by the wind tunnel at Mach numbers ranging up to 0.3, with the Reynolds numbers based on airfoil chord ranging from 1.0×10^5 to 1.0×10^6. The turbulence intensity at outlet of the wind tunnel is keep below 1%.

A SD2030 airfoil (with 4% camber, 8% thickness) with a 150 mm chord and 300 mm span, is placed into the core of an open jet of the tunnel exit which is shown in Fig. 1. The airfoil is mounted onto a plexiglass disk, which allows tuning the angle of attack α from -5 to +5 degree as shown in figure 1(a).

An unequal spacing linear microphone array with 31 microphones (Fig. 1(b)) was used to identify the sound source around airfoil and to analysis the noise strength and spectra. The array was placed just underneath the airfoil about 0.405 m and the centre of the array was placed underneath the centre of airfoil. The all microphone with its diaphragm is mounted on a large, hard reflecting surface so that the sound pressure levels obtained will be augmented over the whole spectrum, up to the frequency at which incident and reflected waves interfere, by a factor of 2 (6 dB) (as shown Fig. 1(a)).

The ¼ inch capacitive microphones produced by BSWA Company are used. Frequency range of this type microphone is from 20 Hz to 20 kHz in free field, and sound pressure levels up to 168 dB. The sensitivity is 5 mV/Pa. The microphone has an operating temperature range of –50 to +110 degree Celsius, and with a main ambient temperature coefficient of 0.01 dB/K and a main ambient pressure coefficient of -10-5 dB/Pa. The ¼ inch measuring microphone preamplifier is a high-impedance transducer for condenser measuring microphone cartridges. It permits a wide-band measurements and sound level measurements with a dynamic range from 17 up to 168 dB. Its frequency range is from 1 Hz to 1 MHz. The microphone preamplifiers were connected to the BBM data acquisition system. The maximum sampling rate of the BBM system was 102.4 KHz. All microphone signals were simultaneously sampled with an AD conversion of 16-bit at a sampling frequency of 32768 Hz. The recording time for one measurement was 10 s. The calibration constants of microphones were

obtained by using a 1000 Hz single frequency standard sound source before the measurement started.

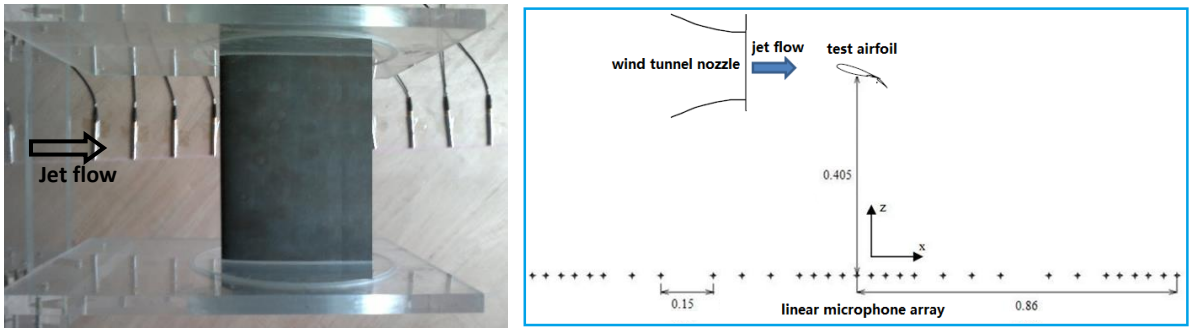

(a) SD2030 airfoil and measure microphones *(b) test fit*

Figure 1. Microphone array and the test fit

3 SEPARATION AND QUANTIFICATION METHOD OF NOISE SOURCES

Despite the fact that microphone measurement is complicated by reflections of the sound waves in wind tunnel or indoor test beds, the applications of more and more microphone arrays in wind tunnels and test room have proven their ability to quantify differences in sound source levels for test model, especially using the deconvolution technique (DAMAS, Clean, et al). In order to separate and quantify the airfoil leading-edge and trailing-edge noise source in the hard-walled room test of the open jet wind tunnel, the microphone placement, the array design, and the removing of background noise are all expressly investigated and analyzed in this paper.

3.1 Indoor Microphones Placement

It should be firstly noted that sound source localization of the beamforming is based on the incident sound wave, and ill-suited placement of microphone array may introduce ambiguities into sound source localization measurements in the hard-walled room test. If beamforming is used in indoor test bed, the microphone should be put in the direct-field or free-field to estimate the acoustic radiation of noise source. As indicated by Soderman and Allen, the direct field is the region near the source where the source levels are strong enough to dominate the reverberant sound caused by any reflections. In the acoustic field which there exist sound reflection such as in hard-walled test room, the direct field could be determined by the reverberant radius $r_{H,}$ it defines the distance from a source where the pressure level of the direct sound and the diffuse noise field are equal. The following equation defines r_H for an omnidirectional source and microphone:

$$r_H = 0.057\sqrt{V/T_{60}} \tag{1}$$

where r_H in m is a function of the room volume V in $m^3$and the reverberation time T_{60} in s. The signal of a microphone positioned at a distance from the sound source smaller than the reverberant radius is dominated by the sound source. Microphones at larger distances, however, are dominated by the diffuse field or background noise.

The reverberation time T_{60} is a measure to describe the absorption of acoustic energy in an enclosure. It is the time during which the sound pressure level drops by 60 dB after a sound source was suddenly turned off. A strong absorption or a short reverberation time causes low

background noise levels and increases the acoustic reverberant radius r_H. The method as suggested by Böhning et al was used in this study to measure the reverberation time of the cascade test bed room with an omni-directional sound source. Figure 2 shows the results for the one-third octave bands between 100 Hz and 10 kHz.

From Fig. 2(a), it could be seen that the reverberation time for frequencies higher than 500 Hz is below 0.5 s. The corresponding reverberation radius was calculated with an estimated volume of the room V = 8.4m ×6m ×2.68 m and is plotted as a function of frequency in figure 2(b). It could be seen that the reverberant radius is in 0.7 m to 1.1 m. It can be concluded that when the distances of all microphones of array to the source is smaller than 0.95m, the array signals are located in the direct field in the frequency range of 400 Hz-10000 Hz.

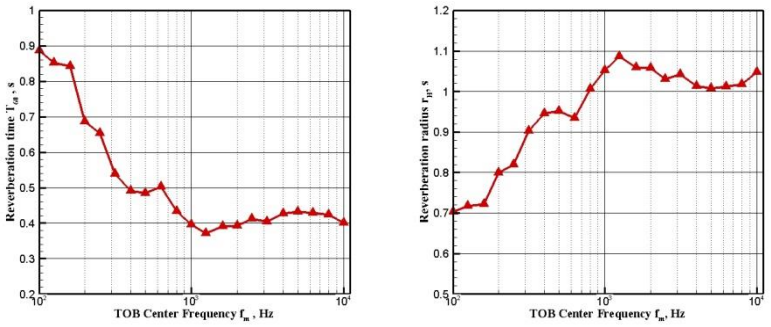

(a) *(b)*

Fig.2 Reverberation time and reverberation radius in the test bed as function of 1/3-octave band centre frequencies.

It should be noted that microphones too close to the sound source also cause errors. A microphone placed in the acoustic near-field, could suffer significantly from pressure fluctuations which do not propagate as sound, and the signals of the microphone will not be representative of the sound propagating to far-field, which is what we are usually trying to simulate. To avoid this effect, it is generally found that the source-to-microphone distance should be at least half of one acoustic wave length(keep the microphone in the acoustic far-field, beyond the hydrodynamic fluctuation close to the source.) and two source dimensions(keep the microphone in the geometrical far-field). In the far-field, the acoustic pressure decays as 1/r (where r is the distance measured from source center), and according this relation to build up steering vector for the conventional beamforming.

As shown in Figure 1(b), the microphone array is placed just underneath the airfoil about 0.405 m, and the center of the array was placed underneath the center of airfoil. The closest microphone in the array to noise source is about 0.405m, that is the lowest frequency of the source which is in the acoustic far-field is 420Hz. The farthest microphone to noise source in the array is about 0.95m, that is the frequency range of the source which is in the direct field according to figure 2(b) is in 400 Hz-10000 Hz.

3.2 Microphone Array Design

The deconvolution array data algorithm, Clean-SC, is used in this paper to separate and quantify the airfoil leading-edge and trailing-edge noise source. It is well known that the deconvolution algorithm is based on the source identification results using classical beamforming. The performance of a microphone array beamforming is the beam pattern, which is the spatial response of the array beam forming to a mono-pole wave. An array beam

pattern comprises a main lobe or beam and a number of smaller side lobes on either side of the main beam. The width b of the main lobe at 3 dB below the peak decides the spatial resolution of the array and it puts a limit on the lowest frequency of the array analysis, where two adjacent sources can be resolved. The beam width b of the array is proportional to the wavelength λ, the distance between the array and the source r and inversely proportional to the diameter of the array d and the emission angle θ:

$$b \approx \frac{\lambda r}{d \sin^2 \theta} \tag{2}$$

The array is designed as shown in figure 1(b) in this experiment. The length of the linear array was 1.72 m, the max space between two adjacent microphones was 0.15 m and the minimum space was 0.075 m. As shown in figure 1(b), if the origin of coordinate is located on the center of linear array, the investigated noise sources, leading-edge source is located on (-0.07 m, 0.405 m), trailing-edge noise source is located on (0.08 m, 0.405 m), and the loudest background noise which is from wind tunnel open jet exit, is located on (-0.225 m, 0.405 m). The emission angle is about 90 degree and the distance r is about 0.405m, and the diameter is limited in 1.72m. The array beam pattern was calculated from the measured signals using a Fast Fourier Transform Algorithm (FFT), a Hanning window with a block size of N = 8196 samples and a 50% overlap had been used.

The beamforming of present array is shown in figure 3. It could be seen that the noise source which is depart from other source 0.1m with the frequency above 1000Hz could been identified using resent linear array.

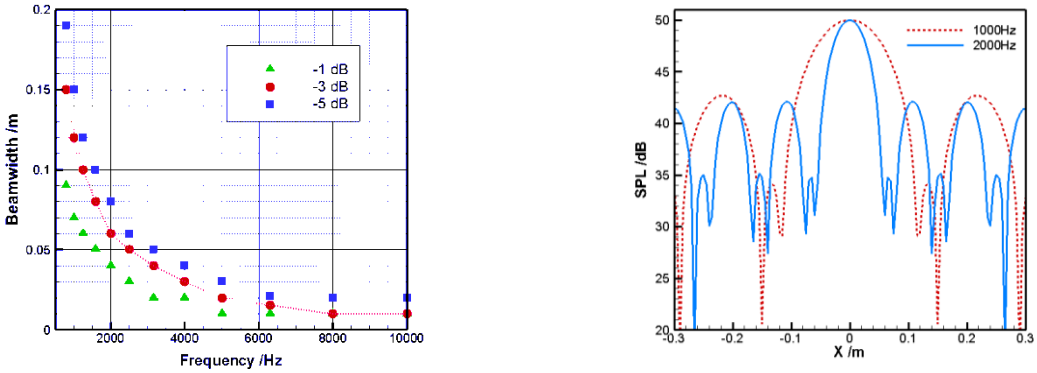

(a) beam width *(b) beam pattern for 1KHz and 2KHz sources*

Figure 3. The pattern of the linear array as a function of the frequency

3.3 The removing of background noise

The background noise produced by the wind tunnel exit jet is a troublesome noise in the open jet wind tunnel test, and this background noise increases with the increasing of flow velocity. Especially, the wind tunnel jet noise is often spatially coherent with the investigated noise source, such as LE and TE noise of airfoil. Therefore, removing the effect of the background noise is very important in the separation and quantification of airfoil LE and TE noise source.

The Diagonal Removal Method (be called as DR for short) which is firstly proposed by Mosher and Dougherty is a frequently-used method to remove background noise. However, the DR method could not improve the Cross Spectral Matrices(*CSM*) of microphone array when the background noise is spatially coherent with the investigated noise source. A new method to remove the spatially coherent background noise based on the deconvolution array

data algorithm, Clean-SC method, is proposed in this study. Firstly, the *CSM* of background noise (wind tunnel open jet noise), noted as CSM_{back} is obtained using the separate blowing of wind tunnel without test airfoil. Then, the airfoil noise test is carried out. After the test, the microphone array data is processed according to the following steps to get the information of target noise source.

Step 1: classical beamforming is firstly obtained as:

$$Y_n^{(0)} = \vec{V}_n'^{*} \cdot \overline{\mathbf{D}}^{(0)} \cdot \vec{V}_n' \tag{3}$$

here, $\mathbf{D}^{(0)} = \mathbf{CSM}$ is the initial value, and

$$\overline{\mathbf{D}}^{(i)} = \mathbf{D}_{diag=0}^{(i)}, \ \vec{V}_n' = \vec{v}_n' \Big/ \left(M^2 - M\right)^{0.5} \tag{4}$$

$\vec{v}$ is the Steering vector of microphone array.

Step 2: to determine the position and level of background noise:

$$Y_{back}^{(i)}, \quad i = Nback$$

Step 3: to do the computation of Clean iteration using Clean-SC.

Step 4: to obtain the target noise source with the calculation of

$$Z_n = \sum_{i=1}^{Nback-1} O_n^{(i)} + \sum_{i=Nback+1}^{I} O_n^{(i)} + Y_n^{(I)} \tag{5}$$

Where, $0_n^{(i)}$ is the results from Clean-SC, and,

$$Y_{n,noback} = Y_n - \vec{V}_n'^{*} \cdot \mathbf{CSM}_{back} \cdot \vec{V}_n' \tag{6}$$

4 TEST RESULTS

4.1 Background noise and its removing

Figure 4 shows the classical beamforming results of the wind tunnel exit jet noise (shown as WT noise in figures) without test airfoil. It could be seen that the wind tunnel exit jet noise is a distributional noise which is spread down the exit and it would contaminate the test airfoil noise source which is located on the jet-core region.

Figure 5 is the classical beamforming results and the deconvolution beamforming results with the removing background noise for airfoil test at airflow speed of 47m/s. It could be seen that, besides the same background noise source as in the figure 4, the LE noise source and TE noise source of airfoil are appeared in these beamforming results(shown as LE and TE noise in figures). It is obvious that the LE noise source and TE noise source are contaminated by the wind tunnel jet noise in the classical beamforming results(figure 5(a)).

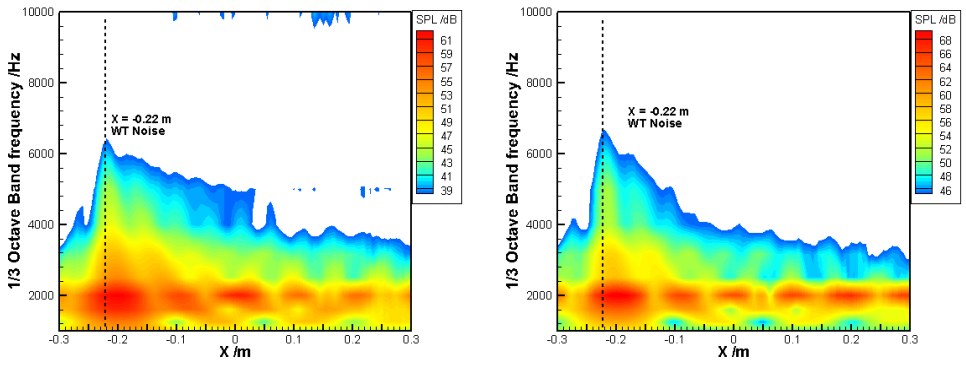

(a)U = 22 m/s *(b)U = 28 m/s*

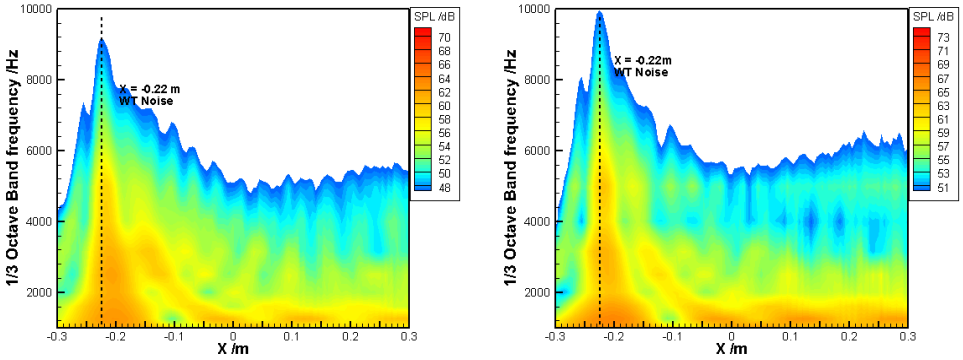

(c)U = 38 m/s *(d)U = 47 m/s*

Figure 4 classical beamforming results of the wind tunnel exit jet noise

In order to remove the effect of background noise on the airfoil LE and TE edge noise, and to eliminate the effect of the beamforming side-lobe on the noise source, the method to remove the spatially coherent background noise based on the Clean-SC method proposed in this study is used (indicated in equations (3)~(6)). The figure 5(b) is the deconvolution beamforming results with the present array data reduction method for the same test as the figure 5(a). It could be seen that, the very "clean" noise source identification is obtained with the present array data reduction method.

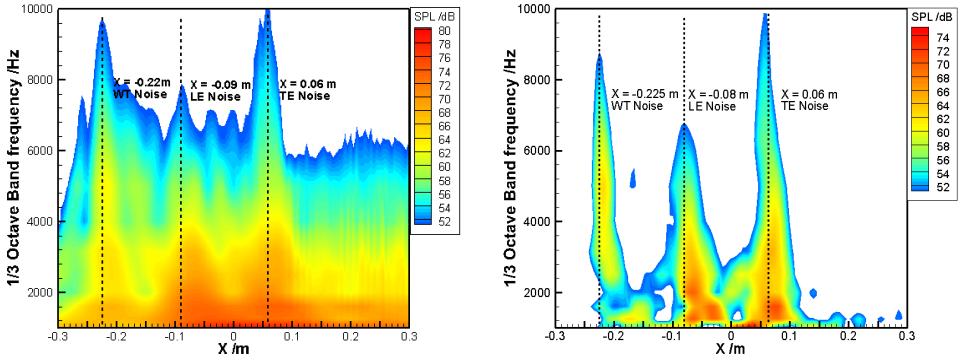

(a) classical beamforming *(b) beamforming removing background noise*

Figure 5 The beamforming results of the airfoil test in the open jet wind tunnel(U = 47 m/s)

4.2 Separation and Quantification of Airfoil LE and TE Noise Source

The SD2030 airfoil LE and TE noise are tested with different flow velocities and different attack angles. The flow speeds are of U=22 m/s, 28 m/s, 38 m/s and 47 m/s, and the corresponding Reynolds numbers based on the airfoil chord are respectively of 218543, 278146, 377483 and 466887. The inflow attack angles of airfoil are of -10 °, -5 °, 0 °, +5 ° and +10 °. Figure 6 to 10 show the beamforming results.

It could be seen from figure 6 to 10 that the wind tunnel jet noise level(WT noise) is almost same at the same airflow speed in different test case(different airfoil attack angle). The LE noise SPL increases a little at the positive attack angle, and decrease a little at the negative attack angle, and the TE noise level vary little with the change of attack angle. In addition, comparing with the positions of the loudest level of LE and TE source at attack angle of 0 degree, the position of the loudest level of LE and TE noise sources move downstream about

1 centimetre at attack angle of +10 degree, and move upstream about 1 centimetre at attack angle of -10 degree.

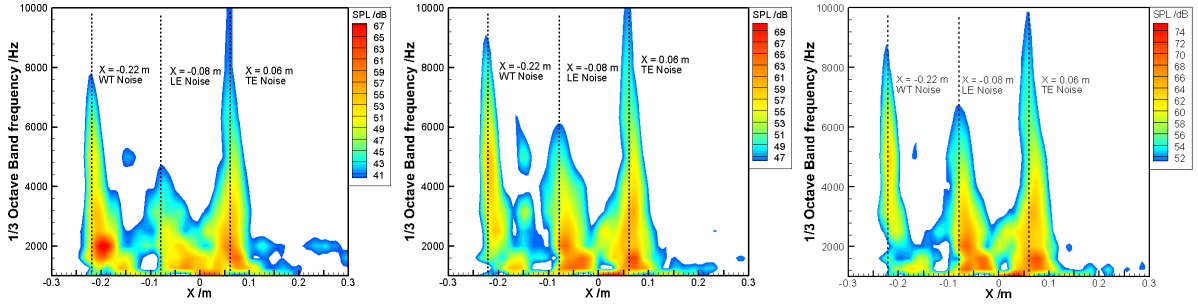

(a)U=28 m/s *(b)U=38 m/s* *(c)U=47 m/s*

Figure 6 Airfoil LE and TE noise test results for the attack angle of 0 degree

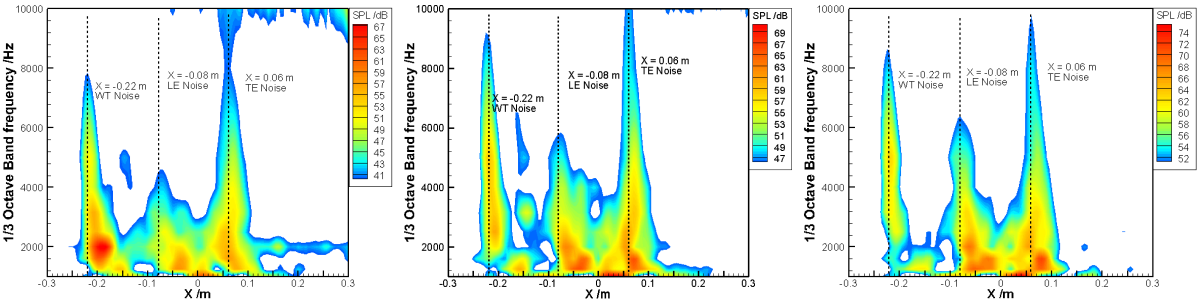

(a)U=28 m/s *(b)U=38 m/s* *(c)U=47 m/s*

Figure 7 Airfoil LE and TE noise test results for the attack angle of +5 degree

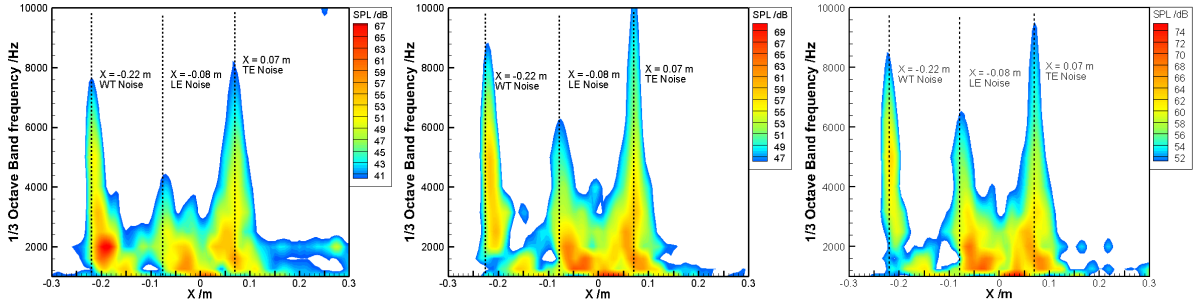

(a)U=28 m/s *(b)U=38 m/s* *(c)U=47 m/s*

Figure 8 Airfoil LE and TE noise test results for the attack angle of +10 degree

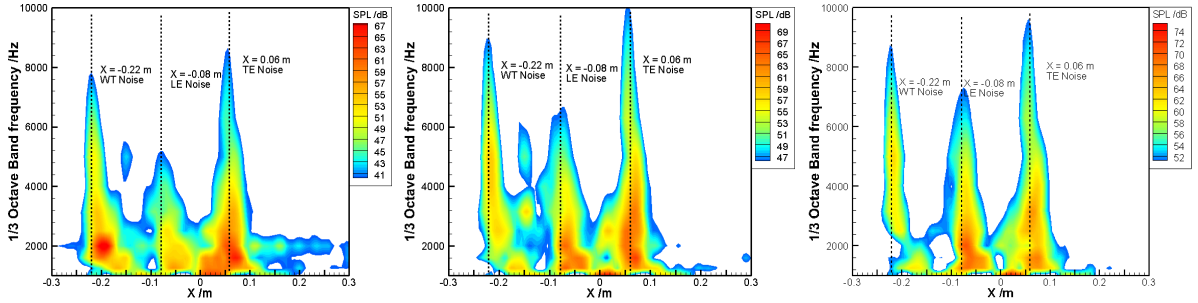

(a)U=28 m/s *(b)U=38 m/s* *(c)U=47 m/s*

Figure 9 Airfoil LE and TE noise test results for the attack angle of -5 degree

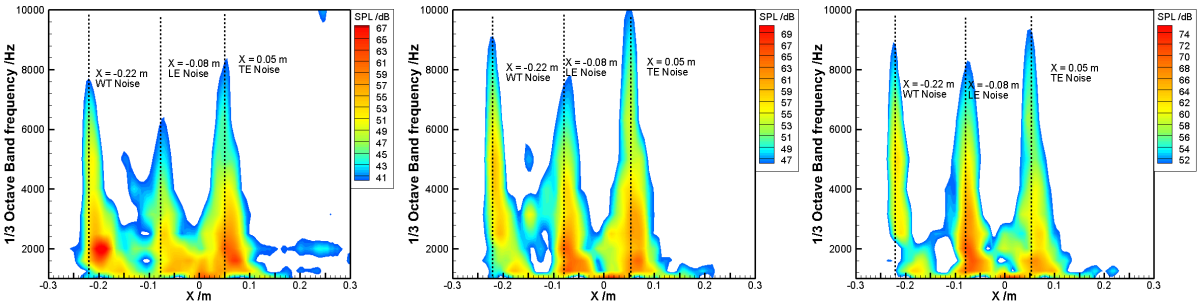

(a)U=28 m/s *(b)U=38 m/s* *(c)U=47 m/s*

Figure 10 Airfoil LE and TE noise test results for the attack angle of -10 degree

4.3 The 1/3 octave spectral of LE noise

It could be seen from the beamforming results that the main lobe of LE and TE all have some width in space. The magnitude of the LE and TE noise should be the sum of sound level in specified space. In this study, the sound pressure level of LE and TE noise are calculated by the following equation,

$$L_{LE} = 10 \cdot \lg \left(\frac{\sum_{n=N_{\min}}^{N_{\max}} 10^{0.1 L_n}}{N_{\max} - N_{\min} + 1} \right) \tag{7}$$

Ln is the sound pressure level at position n. Suppose that the LE and TE noise source center is at the position of maximum sound pressure level (OASPL in frequency range of 1000Hz to 10000Hz), N_{min} is the upstream position where the OASPL is smaller of 3 dB than the maximum OASPL, and N_{max} is the downstream position where the OASPL is smaller of 3 dB than the maximum OASPL.

Figure 11 shows the 1/3 octave spectral of LE noise SPL at different airflow speed with different attack angle. It is obvious that the LE sound pressure level is increased with the increase of the airflow speed. It could also be seen from these figures that the LE noise SPL is decreased with increase of attack angle. The largest difference of the SPL between LE noise at -10degree and +10degree is about 5dB.

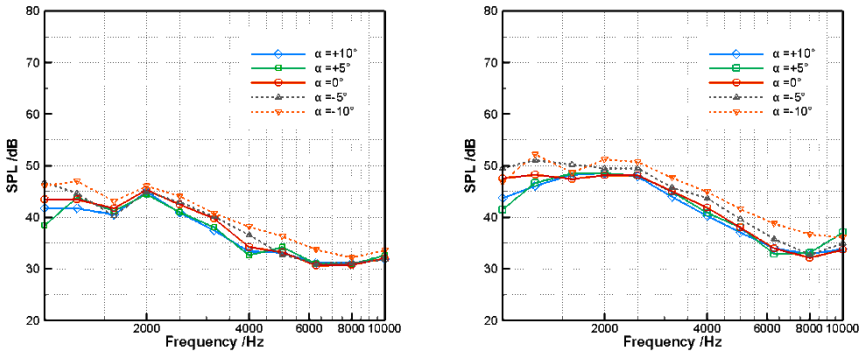

(a)U=22 m/s *(b)U=28 m/s*

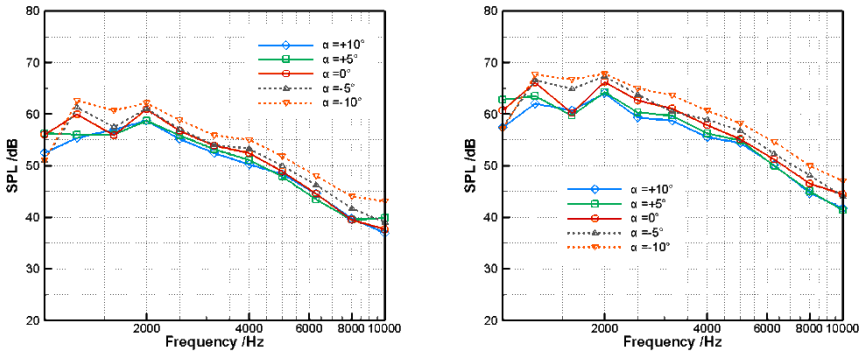

(c)U=38 m/s *(d)U=47 m/s*

Figure 11 The 1/3 octave spectral of LE noise

Figure 12 presents the Overall Sound Pressure Level(OASPL) of LE noise in the frequency range of 1000Hz to 10000Hz vary with the airflow speed. The results at figure 12 are all normalized by the OASPL at the airflow speed of 22m/s. It could be seen that the OASPL of LE noise varies with the airflow speed by the exponential relationship with the index range of 5.965~6.486. The index is decreased with the increase of the attack angle. This results is similar as the relation given by Amiet about the LE noise varies which the strength of LE noise varies with the flow speed by the exponential relationship with the index range of 5~6.

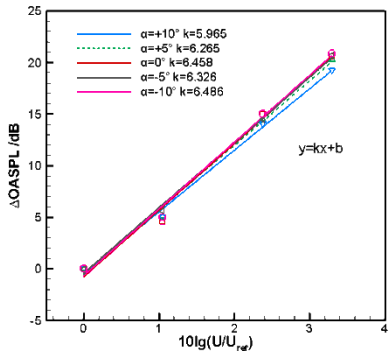

Figure 12 The Overall Sound Pressure Level(OASPL) of LE noise vary with the airflow speed

4.4 The 1/3 octave spectral of TE noise

Figure 13 shows the 1/3 octave spectral of TE noise SPL at different airflow speed with different attack angle. It is obvious that the TE sound pressure level is increased with the increase of the airflow speed. However, the TE noise has a complicated relation with the airfoil attack angle. It could be seen from this figure that the TE noise SPL is largest at the attack angle of -5degree in the test flow speed range, especially at the frequency range above 2000Hz.

Figure 14 presents the Overall Sound Pressure Level(OASPL) of TE noise in the frequency range of 1000Hz to 10000Hz vary with the airflow speed. The results at figure 14 are all normalized by the OASPL at the airflow speed of 22m/s. It could be seen that the OASPL of TE noise varies with the airflow speed by the exponential relationship with the index range of 3.138~6.244. The index is increased with the increase of the attack angle.

Brooks's experimental research on the TE noise indicated that the strength of TE noise varies with the flow speed by the exponential relationship with the index range of 5~5.3 at the

attack angle of 0 degree. Most theoretical analysis for the TE noise at the attack angle of 0 degree also indicated that TE noise varies with the flow speed by the exponential relationship with the index range of 5~6. The present study shows a similar result as the previous results which the TE noise varies with the flow speed by the exponential relationship with the index range of 5.1 at the attack angle of 0 degree. However, when the attack angle of airfoil deflects 0 degree, the relation of TE noise level with the airflow speed is complex.

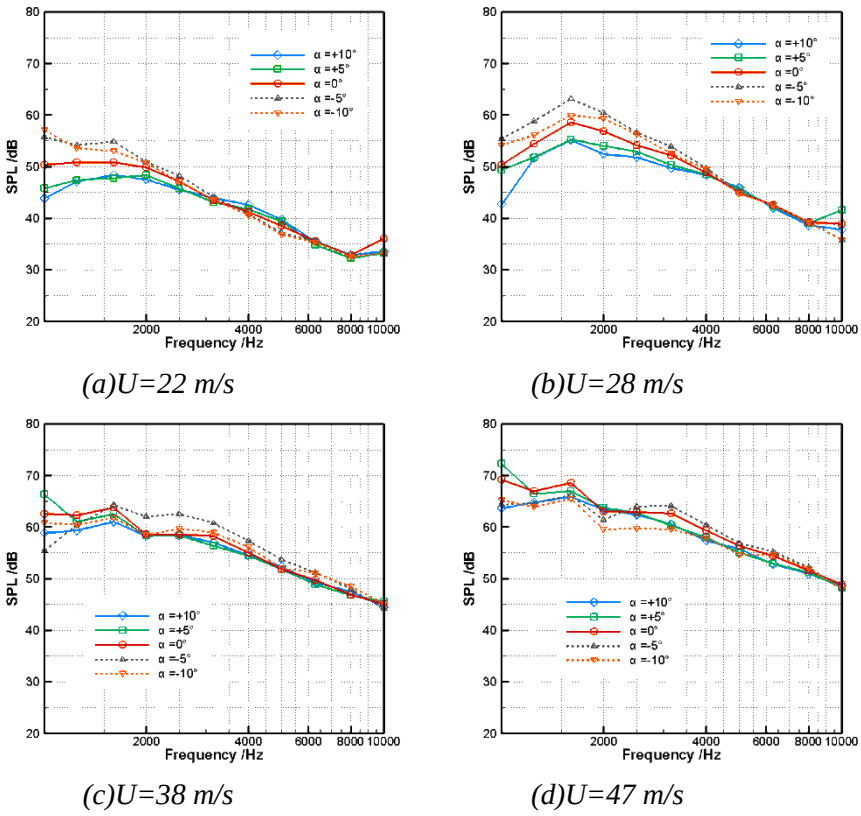

(a)U=22 m/s *(b)U=28 m/s*

(c)U=38 m/s *(d)U=47 m/s*

Figure 13 The 1/3 octave spectral of TE noise

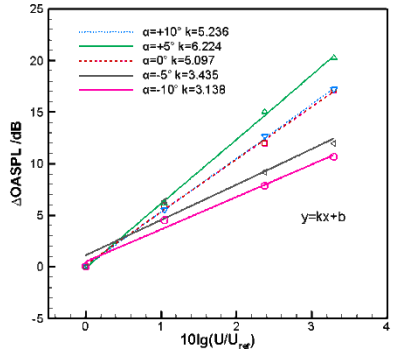

Figure 14 The Overall Sound Pressure Level(OASPL) of TE noise vary with the airflow speed

5 CONCLUSIONS

The source identification technology based on the Clean-SC approach with microphone array was successfully used in this study to separate and quantify airfoil LE and TE noise source in

an indoor open jet wind tunnel test. Clear and quantitative sound radiation results from the airfoil LE and TE noise source are obtained. According to this study, some conclusions can be drawn below.

(1)The present test results show that wind tunnel noise source, the leading edge noise source and trailing edge noise source could be identified clearly with the using of special designed linear microphone array. With the Clean-SC approach and with the correction of reverberation and shear layer, the background noises produced by the wind tunnel exit jet is successfully removed using the removing of Cross Spectral Matrices(CSM_{back}) of the background noises from the *CSM* of measurement noise.

(2) It is obvious that the LE and TE sound pressure level are increased with the increase of the airflow speed. It was found that the LE noise SPL of airfoil is decreased with increase of attack angle. The largest difference of the SPL between LE noise at -10degree and +10degree is about 5dB. However, the TE noise has a complicated relation with the airfoil attack angle. It was found that the TE noise SPL is largest at the attack angle of -5degree in the test flow speed range, especially at the frequency range above 2000Hz.

(3)There is a good coincidence between present test results and classical aeroacoustic theory for the LE and TE edge noise at the attack angle of zero degree. It is found that overall sound pressure level (OASPL) varies approximately as $U^{6.5}$ and $U^{5.1}$(U is the mean flow velocity) for the leading edge noise and trailing edge noise respectively when flow attack angle is zero degree.

(4) The influence of the flow attack angle on the trailing edge noise is greater than that on leading edge noise. It is found that the OASPL of LE noise varies with the airflow speed by the exponential relationship with the small index range of 5.965~6.486, and the OASPL of TE noise varies with the airflow speed by the exponential relationship with a very large index range of 3.138~6.244.

ACKNOWLEDGEMENT

The present work is supported by the National Natural Science Foundation of China (Grant No.51276149 and Grant No.51476134), the European Union and China collaborative project in aviation - IMAGE project (Contract No. 688971-IMAGE-H2020MG-2014-1015688971). The authors also gratefully acknowledge the support of the State Key Laboratory of Aerodynamics (Grant No.SKLA20160201), the Key Laboratory of Aerodynamic Noise Control of China Aerodynamics Research and Development Center (Grant No.ANCL20160102).

REFERENCES

1. Curle, N., 1955. The influence of solid boundaries upon aerodynamic sound. Proc. Roy. Soc. (London) A321, 505-514.
2. Powell,A., 1960. Aerodynamic noise and the plane boundary. J. of the Acoustical Society of America, 32, 982-990.
3. Ffowcs Williams,J.E. and Hall,L.H., 1970. Aerodynamic sound generation by turbulent flow in the vicinity of a scattering half plane. J. Fluid Mech., 40,4 657-670.
4. Crighton,D.G. and Leppington,F.G., 1970. Scattering of aerodynamic noise by a semi-infinite compliant plate. J. Fluid Mechanics, 43, 721-736
5. Crighton,D.G., 1972. Radiation from vortex filament motion near a half plane. J. Fluid Mechanics, 51,2,357-362

6. Chandiramani,K.L., 1974. Diffraction of evanescent waves, with application to aerodynamically scattered sound and radiation from unbaffled plates. J. of the Acoustic Society of America, 55,1, 19-29
7. Levine, H., 1975. Acoustical diffraction radiation. Philips Research Report, 30, 240-276
8. Howe,M.S., 1975. The generation of sound by aerodynamic sources in an inhomogeneous steady flow. J. Fluid Mechanics, 67,3, 597-610
9. Howe,M.S., 1976. The influence of vortex shedding on the generation of sound by convected turbulence. J. Fluid Mechanics, 76,4, 710-740
10. Chase,D.M., 1972. Sound radiated by turbulent flow off a rigid half-plane as obtained from a wavevector spectrum of hydrodynamic pressure. J. of the Acoustic Society of America, 52,3,1011-1023
11. Chase,D.M., 1975. Noise radiated from an edge in turbulent flow. AIAA J., 13,8, 1041-1047
12. Davis,S.S., 1975. Theory of discrete vortex noise. AIAA J., 13,3, 375-380
13. Howe,M.S., 1978. A review of the theory of trailing edge noise. J. Sound and Vibration, 61,3 437-465
14. Ji Liang, Experimental and numerical study on mechanism and suppression method of turbo-machinery broadband noise[D]. Ph.D thesis, Northwestern Polytechnical University. 2016.
15. J. Billingsley, "An acoustic telescope," Aeronautical Research Council ARC 35/364. 1974.
16. Ulf Michel, HISTORY OF ACOUSTIC BEAMFORMING, Berlin Beamforming Conference (BeBeC2006), Nov.21-22,2006, Berlin, Germany.
17. D. H. Johnson, D. E. Dudgeon, "Array signal processing: Concepts and techniques" PTR Prentice Hall, Englewood Cliffs, New Jersey, 1993.
18. R. P. Dougherty and Robert W. Stoker, "Sidelobe suppression for phased array aeroacoustic measurements." AIAA-1998-2242, 4th AIAA/CEAS Aeroacoustics Conference, Toulouse, France, June 2-4, 1998
19. S. Brühl and A. Röder, "Acoustic noise source modelling based on microphone array measurements," J. Sound and Vibr. 231(3), 611-617, 2000.
20. T. Brooks, W. Humphreys, "A Deconvolution Approach for the Mapping of Acoustic Sources (DAMAS) Determined from Phased Microphone Arrays." AIAA-2004-2954, 10th AIAA/CEAS Aeroacoustics Conference , Manchester, Great Britain, May 10-12, 2004
21. T. Brooks and W. Humphreys, "Three-Dimensional Applications of DAMAS Methodology for Aeroacoustic Noise Source Definition." AIAA-2005-2960, 11th AIAA/CEAS Aeroacoustics Conference, Monterey, California, May 23-25, 2005
22. T. Brooks and W. Humphreys, "A deconvolution approach for the mapping of acoustic sources (DAMAS) determined from phased microphone array," J. Sound and Vibr. 294(4-5), 856-879, 2006.
23. Sijtsma, P., CLEAN based on spatial source coherence[R]. Germany: NLR, 2007, TP-2007-345.
24. T. Brooks, W. Humphreys, "Extension of DAMAS Phased Array Processing for Spatial Coherence Determination (DAMAS-C)" AIAA-2006-2654, 12th AIAA/CEAS Aeroacoustics Conference, Cambridge, Massachusetts, May 8-10, 2006
25. R. P. Dougherty, "Extensions of DAMAS and Benefits and Limitations of Deconvolution in Beamforming." AIAA-2005-2961, 11th AIAA/CEAS Aeroacoustics Conference, Monterey, California, May 23-25, 2005
26. Suzuki, Generalized Inverse Beamforming Algorithm Resolving Coherent/Incoherent, Distributed and Multipole Sources, AIAA paper 2008-2954, 2008.